Changes of the thermodynamic parameters in failure conditions of the micro-CHP cycle

ROBERT MATYSKO[*]
JAROSŁAW MIKIELEWICZ
EUGENIUSZ IHNATOWICZ

The Szewalski Institute of Fluid Flow Machinery of Polish Academy of the Sciences, Fiszera 14, 80-231 Gdańsk, Poland

Abstract   The paper presents the calculations for the failure conditions of the ORC (organic Rankine cycle) cycle in the electrical power system. It analyses the possible reasons of breakdown, such as the electrical power loss or the automatic safety valve failure. The micro-CHP (combined heat and power) system should have maintenance-free configuration, which means that the user does not have to be acquainted with all the details of the ORC system operation. However, the system should always be equipped with the safety control systems allowing for the immediate turn off of the ORC cycle in case of any failure. In case of emergency, the control system should take over the safety tasks and protect the micro-CHP system from damaging. Although, the control systems are able to respond quickly to the CHP system equipped with the inertial systems, the negative effects of failure are unavoidable and always remain for some time. Moreover, the paper presents the results of calculations determining the inertia for the micro-CHP system of the circulating ORC pump, heat removal pump (cooling condenser) and the heat supply pump in failure conditions.

Keywords: Micro-CHP system; Transient model; Failure states; Multifuel boiler system; Heating system

---

[*]Corresponding Author. E-mail: matyskor@imp.gda.pl

Nomenclature

A	–	surface
B	–	calorific value, J/kg
c_p	–	specific heat at constant pressure, J/(kgK)
c_v	–	specific heat at constant volume, J/(kgK)
CHP	–	combined heat and power
D	–	derivative gain
d	–	mathematical operator of differentation
g	–	gravitational acceleration, m/s^2
h	–	enthapy, kJ/kg
H	–	pumping head
I	–	integral gain
i	–	control signals
k	–	overall heat transfer coefficient, W/(m^{2}K)
L	–	heat exchanger's length, m
M	–	mass, kg
$\dot{m}$	–	mass flow, kg/s
ORC	–	organic Rankine cycle
P	–	power, proportional gain, W
PID	–	proportional integral derivative controller
PLC	–	programable logic controller
p	–	pressure, Pa
$\dot{Q}$	–	volumetric flow rate, m^3/s
s	–	Laplace operator
T	–	temperature, °C
t	–	time, s
x	–	drynees factor

Greek symbols

λ	–	thermal conductivity, W/(mK)
ρ	–	mass density, kg/m^3
α	–	heat transfer coefficient between fluid and wall surface, W/(m^{2}K)
δ	–	wall thickness, mm

Subscripts

b	–	boiling
hfe	–	hfe7100 working fluid
ins	–	insulation
in	–	input
c	–	condensation
l	–	liquid
n	–	control panel
out	–	output
ol	–	thermal oil

p	–	initial condition, measuring signal
$radiator$	–	thermal radiator
$water$	–	cooling water
v	–	vapour
x	–	drynees degree

1   Introduction

Thermal cycles are equipped with automatic control systems that enable stable operation at variable loads. They also protect other systems from failure. There are many publications available about the operation of the controlling systems of thermal cycles at working conditions. It is easy to find information about the risk and possible consequences of their breakdown. Although, the theoretical studies discuss the physical and mathematical modeling of the dynamic effects occurring in the basic components of the thermal plants (boilers, turbines, heat exchangers, etc.) quite comprehensively [1–4]. There are not many publications about the ORC cycle modelling at failure condition [5–9]. Relatively small amount of available sources of information induced for writing this article and acknowledging the reader with quite new subject [10].

Beside the analysis of the micro-CHP system (Fig. 1) operation at normal condition, the possible failures resulting from the lack of the power supply or the automatic safety valves damage should be considered. Micro-CHP system operates as a free maintenance installation which means that, the final user does not need to know all the details about the system operation because it is equipped with special control systems that turn off the circulation of the system in case of any failure.

To protect the micro-CHP system from the negative effects of the system failure, it is important for the control system to immediately take over all its tasks. Although the control systems are able to quickly respond to micro-CHP systems equipped with inertial systems, they always maintain for a while, under the influence of the negative effects left after the breakdown of the system.

The final user needs only to turn on the system by pushing ON button on the controller or OFF if he wants to turn it off. The user operates also the thermostatic valve mounted on the radiators. The control system of the micro-CHP automatically adjusts the system to the heat demand. In the feedback loop, there is a special control system responding to heating requirements of the individual system components. The micro-CHP system
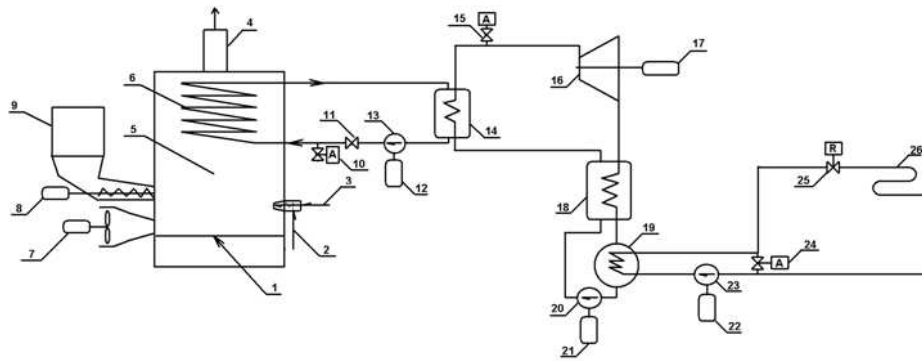
Figure 1. Schematic of the micro-CHP: 1 – multifuel boiler grid, 2 – inlet gas fuel, 3 – inlet of the liquid fuel, 4 – chimney, 5 – combustion chamber, 6 – multifuel boiler coil, 7 – air supply system, 8 – solid fuel screw drive, 9 – solid fuel store, 10 – pressure (relief) valve, 11 – valve, 12 – electric motor oil circulation pump, 13 – oil circulation pump, 14 – evaporator, 15 – pressure relief valve, 16 – microturbine, 17 – electric generator, 18 – regenerator, 19 – condenser, 20 – micro CHP circulation pump, 21 – micro-CHP circulation pump engine, 22 – heating circuit pump engine, 23 – heating circuit pump, 24 – safety valve, 25 – thermostatic valve, 26 – coil of heating system, A – automatic actuator, R – manual controller.

is a very complex system (Fig. 2) used to provide stable thermal parameters. It consists of three subsystems

- multifuel boiler system,

- micro-CHP system,

- heating system.

The systems are equipped with actuators such as valves adjusted, engines (with inverters), and additional protection automation systems.

The PLC control system applied in the micro-CHP systems allows for the internal feedback loops programming. Thanks to that the subsystems can activate with a scheduled delay. The internal control loops consist of

- PID (proportional integral derivative controller) control system for the the heat pump (gives the possibility for the he final user to change the heat flux),

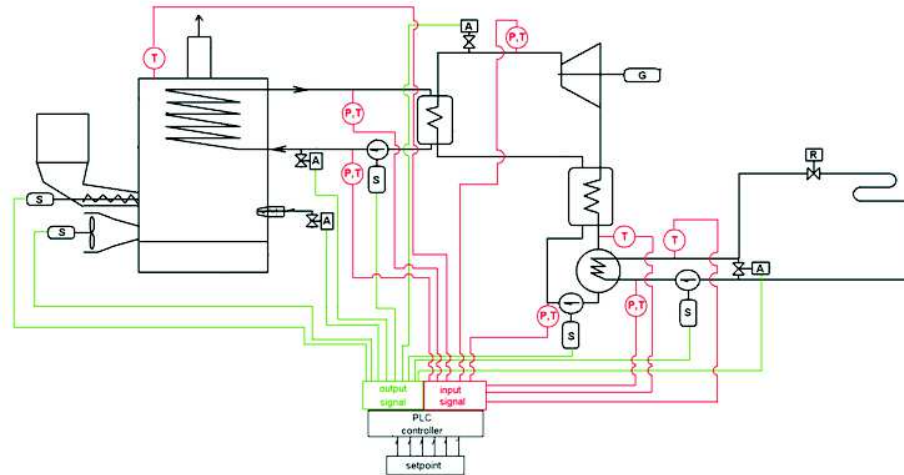- PID control system for the circulation pump working within the micro-CHP cycle,

Figure 2. Signal flow diagram for the continuous control of the micro-CHP system. P – pressure, T – temperature, S – engine, A – actuator, R – manual controller, G – generator, PLC – programmable logic controller.

- PID control system for thermal oil circulation pump and security system (regulating pressure that increases after the emergency shut down of the thermal oil pump),
- PID system controlling the temperature and heat flux in the multifuel boiler.

The aim of the paper is to present the calculations determining the time neccessary for the micro-CHP system inertia to react in case of failure of the ORC circulating pump, heat removal (cooling condenser) circulating pump, and heat supply (heating the evaporator) circulating pump.

2 Subcycle models of the micro-CHP

Assumptions and simplifications adopted in the model describing the failure working conditions:

- lumped-parameter model,
- model describing thermodynamic parameters changes in time (transient model),
- combustion model presenting the convective heat transfer (skipping the processes of the radiative heat transfer),

- ORC system controllers working in a negative feedback loop,

- PID controller manages the pump control cycle with a scheduled delay,

- state variable (fluid mass flow) is used for regulation purposes in failure conditions,

- heaviside step function models the system failure conditions in the steady state,

- the model does not include the boiling process disappearance in the boiler.

- specific heat of the two-phase mixture was determined for the dryness factor $x = 0.5$.

Below presented equations describe the processes present in heat exchangers during the phase change. Figures 3 and 4 illustrate condensation process and boiling process, respectively.
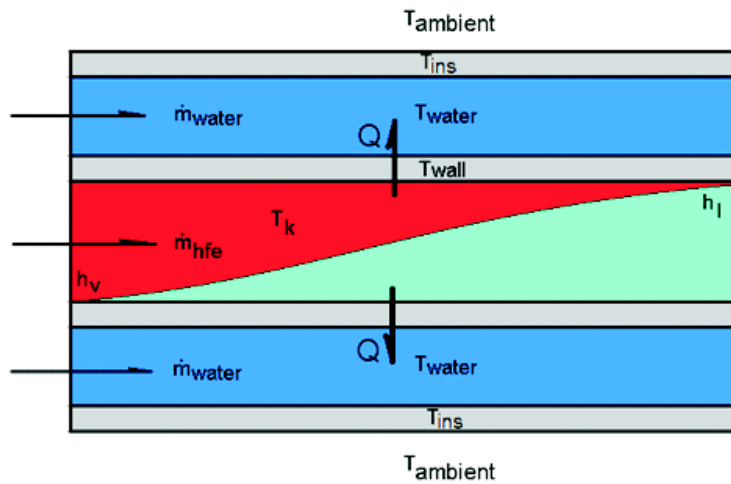
Figure 3. Graphical interpretation of the condensation process in the exemplary heat exchanger.

- Condensation process

$$\frac{dT_k}{dt} = \frac{1}{c_{p,x}M_c}\left[A_{wall}k_{hfe,wall,k}\left(T_{wall} - T_k\right) + \dot{m}_{hfe}\left(h_v - h_l\right)\right] . \qquad (1)$$
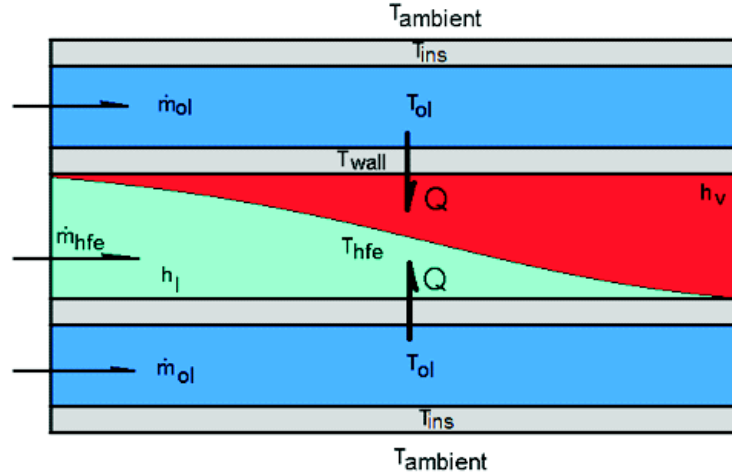
- Heat transfer through the condenser's wall

Figure 4. Graphical interpretation of the boiling process in the exemplary heat exchanger.

$$\frac{dT_{wall}}{dt} = \frac{1}{M_{wall}c_{p,wall}} \Big[A_{wall}k_{hfe,wall}\left(T_k - T_{wall}\right) +$$

$$+ A_{wall}k_{wall,water}\left(T_{water} - T_{wall}\right) \Big] . \qquad (2)$$

- Water cooling

$$\frac{dT_{water}}{dt} = \frac{1}{M_{water}c_{p,water}} \Big[c_{p,water}\dot{m}_{water}\left(T_{water,in} - T_{water}\right) +$$

$$A_{ins}k_{water,ins}\left(T_{ins} - T_{water}\right) + A_{wall}k_{wall,water}\left(T_{wall} - T_{water}\right) \Big]. \quad (3)$$

- Heat transfer through the insulation

$$\frac{dT_{ins}}{dt} = \frac{1}{M_{ins}c_{p,ins}} \Big[A_{ins}k_{water,ins}\left(T_{water} - T_{ins}\right) +$$

$$+ A_{ins}k_{ins,ambient}\left(T_{ambient} - T_{ins}\right) \Big] . \qquad (4)$$

The following equations illustrating the processes undergoing in the evaporator.

- Evaporation process

$$\frac{dT_b}{dt} = \frac{1}{c_{p,x}M_b} \left[A_{wall}k_{hfe,wall,b}\left(T_{wall} - T_b\right) - \dot{m}_{hfe}\left(h_v - h_l\right) \right] . \qquad (5)$$

- Heat transfer through the wall of the evaporator

$$
\begin{aligned}
\frac{dT_{wall}}{dt} = \frac{1}{M_{wall}c_{p,wall}} \big[& A_{wall}k_{hfe,wall}\left(T_b - T_{wall}\right) + \\
& + A_{wall}k_{wall,ol}\left(T_{ol} - T_{wall}\right) \big] \, .
\end{aligned} \tag{6}
$$

- Oil heating

$$
\begin{aligned}
\frac{dT_{ol}}{dt} = \frac{1}{M_{ol}c_{p,ol}} \big[& c_{p,ol}\dot{m}_{ol}\left(T_{ol,in} - T_{ol}\right) + A_{ins}k_{ol,ins}\left(T_{ins} - T_{ol}\right) + \\
& + A_{wall}k_{wall,ol}\left(T_{wall} - T_{ol}\right) \big] \, .
\end{aligned} \tag{7}
$$

- Heat transfer through the insulation

$$
\begin{aligned}
\frac{dT_{ins}}{dt} = \frac{1}{M_{ins}c_{p,ins}} \big[& A_{ins}k_{ol,ins}\left(T_{ol} - T_{ins}\right) + \\
& + A_{ins}k_{ins,ambient}\left(T_{ambient} - T_{ins}\right) \big] \, .
\end{aligned} \tag{8}
$$

In Eqs. (1)–(8), an overall heat transfer coefficient, k, has been adapted to determine the temperature of the wall in the heat exchangers (Fig. 5). Dependencies presented in Eq. (9) were taken into consideration.

$$
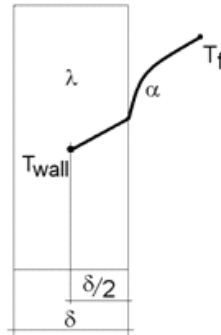\frac{1}{k} = \frac{1}{\alpha} + \frac{\delta}{2\lambda} \, . \tag{9}
$$

Figure 5. A scheme for the designation of the heat transfer coefficient.
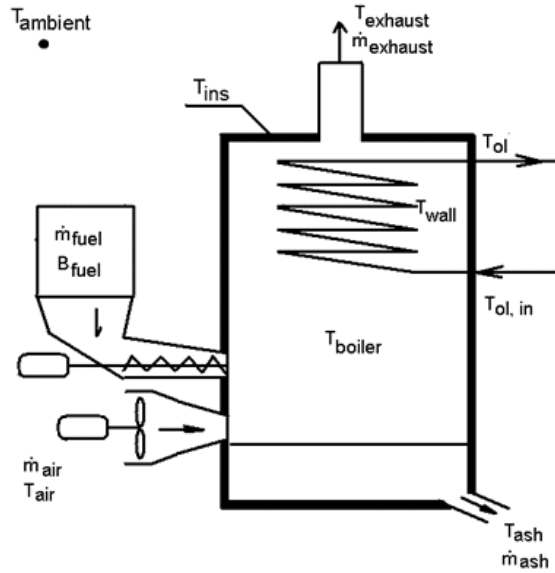
Figure 6. Diagram illustrating the modelled multifuel boiler.

Figure 6 presents the scheme applied for the thermal balance estimation in the boiler, while Fig. 7 introduces the scheme of the heating balance in the utility room. A dynamic model describing the operation of the boiler cycle (indirect evaporator heating system).

- Heat transfer in the thermal oil

$$\frac{dT_{ol}}{dt} = \frac{1}{M_{ol}c_{p,ol}} \left[c_{p,ol}\dot{m}_{ol}\left(T_{ol,in} - T_{ol}\right) - k_{wall,ol}A_{wall,ol}\left(T_{ol} - T_{wall}\right) \right]. \quad (10)$$

- Energy balance for the boiler

$$M_{boiler}c_{p,boiler}\frac{dT_{boiler}}{dt} = \left[\dot{m}_{fuel}B_{fuel} + c_{p,air}\dot{m}_{air}T_{air} + \right.$$
$$+ c_{p,ol}\dot{m}_{ol}\left(T_{ol,in} - T_{ol,out}\right) - k_{ins}A_{ins}\left(T_{boiler} - T_{izol}\right) - \quad (11)$$
$$\left. - c_{p,exhaust}\dot{m}_{exhaust}T_{exhaust} - c_{p,ash}\dot{m}_{ash}T_{ash} \right].$$

- The dynamics of the heat transfer describes equation, showing the cold liquid return from the heating system (Fig. 7)

$$M_{water}c_{p,water}\frac{dT_{water,out}}{dt} = \dot{m}_{water}c_{p,water,out}\left(T_{water,in} - T_{water,out}\right) -$$
$$- k_{radiator,room}A_{radiator}\left(T_{water,out} - T_{room}\right). \quad (12)$$

The dynamics of the heat transferred from the heated room to the environment describes the equation

$$M_{room}c_{p,room}\frac{dT_{room}}{dt} = k_{radiator,room}A_{radiator}\left(T_{water,out} - T_{room}\right) -$$
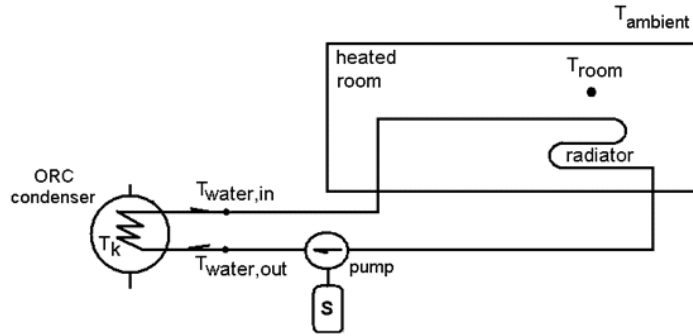$$-k_{room,ambient}A_{ambient}\left(T_{room} - T_{ambient}\right). \tag{13}$$

Figure 7. Diagram presenting the modelled heating system.

Additional equations describing the pumps and micro turbines.

- Pump net power

$$P = \dot{Q}H\rho g. \tag{14}$$

- Pump head

$$H = \frac{p_b - p_k}{\rho g}. \tag{15}$$

- Temperature at the outlet of the micro turbine:

$$T_k = \left[(T_b + 273,15)\left(\frac{p_k}{p_b}\right)^{\frac{\frac{c_{p,v}(T_k)}{c_{v,v}(T_k)}-1}{\frac{c_{p,v}(T_k)}{c_{v,v}(T_k)}}}\right] - 273.15. \tag{16}$$

The equation describing the dependencies of the regulator's functioning

$$P(s) = 0 \leq \left|\left(P + I\frac{1}{s} + Ds\right)(i_n - i_p)\right| \leq \max. \tag{17}$$

Graduate changes have been introduced to the presented control system to simulate the circulation pump power failure (according to Heaviside's step function).

3   The calculations results

All the provided calculations apply to the initial phase of the processes (presented in the Tabs. 1–4) taking place in the ORC cycle subsystems.

Table 1. Initial and boundary conditions adapted to designate the condenser's dynamics.

Agent HFE7100	Cooling water
Initial conditions	
T=10 °C	
Boundary conditions for working fluids at the condenser's outlet	
$T_{in,hfe}$=70 °C	$T_{in,water}$=20 °C
Supplementary data	
$\alpha_{hfe,wall}$ = 2000 W/(m^{2}K); ρ_{wall} = 7900 kg/m^3; $c_{p,wall}$ = 455 J/(kgK); $\alpha_{water,wall}$ = 400 W/(m^{2}K); ρ_{ins} = 60 kg/m^3; $c_{p,ins}$ =0.1 J/(kgK); $\alpha_{air,ins}$ = 10 W/(m^{2}K); λ_{wall} = 58 W/(mK); λ_{ins} = 0.001 W/(mK); δ = 1 mm	

Table 2. Initial and boundary conditions adapted to designate the evaporator's dynamics.

Agent HFE7100	Heating fluid
Initial conditions	
T=10 °C	
Boundary conditions for working fluids at the evaporator's outlet	
$T_{in,hfe}$=70 °C	$T_{in,water}$=20 °C
Additional data	
$\alpha_{hfe,wall}$ = 2704 W/(m^{2}K); ρ_{wall} = 7900 kg/m^3; $c_{p,wall}$ = 455 J/(kgK); $\alpha_{ol,wall}$ = 546 W/(m^{2}K); ρ_{ins} = 60 kg/m^3; $c_{p,ins}$ =0.1 J/(kgK); $\alpha_{air,ins}$ = 10 W/(m^{2}K); λ_{wall} = 58 W/(mK); λ_{ins} = 0.001 W/(mK); δ = 1 mm	

Table 3. Initial and boundary conditions adapted to designate the dynamics of the heated room.

Initial temperature of the system	Temperatures for the steady state		
T_p = 10 °C	T_{boiler} = 195 °C	$T_{in,ol}$ = 175 °C	$T_{out,ol}$ = 185 °C
Additional data			
Coil: $c_{p,ol}$ = 2000 J/(kgK); k_{wall} = 80 W/(m^{2}K); A_{sc} = 350 m^2; M_{wall} = 800 kg; δ = 1 mm Combustion chamber: $c_{p,air}$ = 1005 J/(kgK); $c_{p,exhaust}$ = 1005 J/(kgK); B = 2.5 MJ/kg			

Micro-CHP automatic loop programming is the main issue in the coordination of the systems. Good programming guarantees a quick response of the

Table 4. Initial and boundary conditions adapted to designate the dynamics of the heated room.

Initial temperature	Steady state temperatures		
$T_p = 10$ °C	$T_{water,in} = 67$ °C	$T_{water,out} = 21.2$ °C	$T_{room} = 19.8$ °C
Additional data			
$c_{p,water} = 2000$ J/(kgK); $A = 100$ m²; $k = 200$ W/(m²K); $M = 200$ kg; $A_{ambient} = 5000$ m²; $k_{ambient} = 30$ W/(m²K); $\delta = 1$ mm			

safety system in case of emergency. Figures 8, 9, 10 and 11 show the calculations for the ORC cycle in failure conditions. Calculations are performed for the micro-CHP with and without security system.

Assuming that the output signal comprises from 10 to 90% of the signal value in steady state, the rise time can be appointed. Steady state can be accomplished if the vibrations value is not greater than 2% of setting value.

The rise time in boiler's coil is equal to 0.21 s. The steady state has been attained after 824 s. The minimum value of the steady state is equal to 178 °C and the maximum amounts to 195 °C in nominal conditions. The rise time of the thermal oil at the coil's output equals 1355 s. (Fig. 8, line 2). The steady state has been attained after 2563 s. The minimum value of the steady state is equal to 166 °C and the maximum amounts to 181 °C in nominal conditions. The rise time of the thermal oil in the inlet of the boiler's coil equals 1548 s. (Fig. 8, line 3). The steady state has been attained after 2825 s. The minimum value of the steady state is equal to 160 °C and the maximum amounts to 175 °C in nominal conditions.

The rise time of the heating water at the outlet of the heating room (Fig. 9, line 2) equals 259 s. The steady state has been attained after 472 s. The minimum value of the steady state is equal to 21.4 °C and the maximum amounts to 22.6 °C in nominal conditions. The rise time of the heating room (Fig. 9, line 3) equals 259 s. The steady state has been attained after 472 s. The minimum value of the steady state is equal to 18.7 °C, while the maximum amounts 19.75 °C in nominal conditions.

The rise time of the HFE7100 fluid at boiling point (Fig. 10, line 2) equals 1548 s. The steady state has been attained after 2825 s. The minimum value of the steady state is equal to 160 °C, while the maximum amounts to 175 °C in nominal conditions. The rise time of the HFE7100 fluid in condensation (Fig. 10, line 3) equals 257 s. The steady state has been attained after 460 s. The minimum value of the steady state is equal to
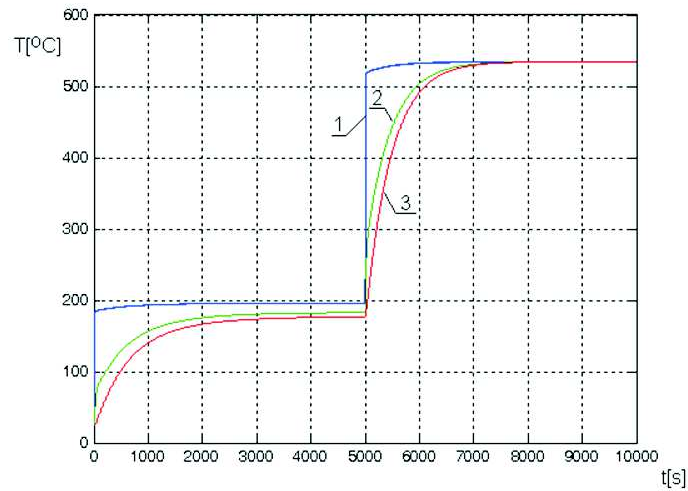
Figure 8. ORC circulation pump failure – results of calculations of temperature in the boiler (failure condition): 1 – the boilers wall; 2 – thermal oil at the outlet of the coil; 3 – thermal oil in the inlet of coil.
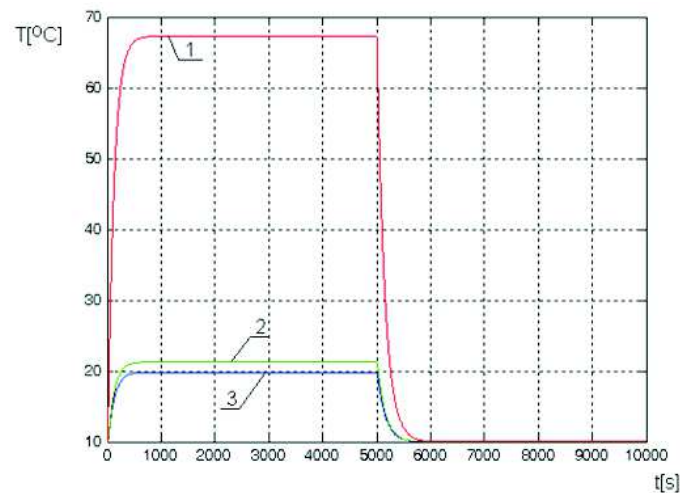

Figure 9. ORC circulation pump failure – temperature in the heated room: 1 – heating water temperature in the inlet of the heated room, 2 – heating water temperature at the outlet of the heated room, 3 – heated room.

62 °C, while the maximum amounts 68 °C in nominal conditions. The rise time of the HFE7100 fluid at boiling point (Fig. 11, line 2) equals 1520 s, for protected ORC cycle. The steady state has been attained after 2745 s. The
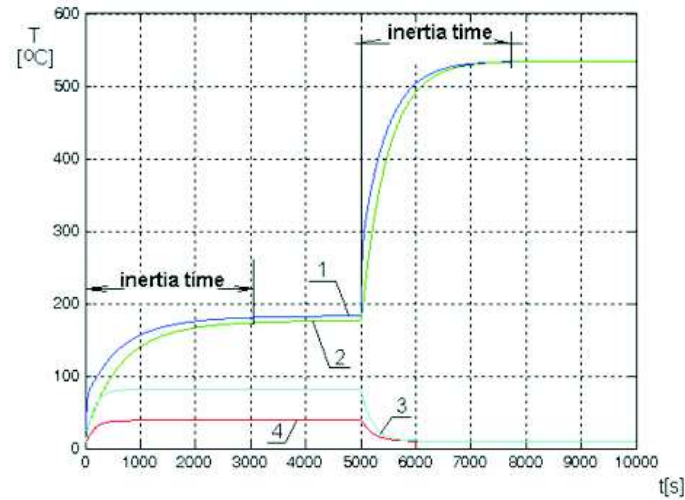
Figure 10. ORC circulation pump failure – temperature calculations for the ORC cycle. 1 – thermal oil temperature in the evaporator's inlet, 2 – HFE7100 fluid temperature in the evaporator, 3 – HFE7100 fluid temperature in the condenser, 4 – cooling water temperature at the condenser's outlet.

minimum value of the steady state is equal to 120 ^{o}C, while the maximum amounts to 124 °C in nominal conditions. The rise time of the HFE7100 fluid in condensation (Fig. 11, line 3) equals 247 s, for protected ORC cycle. The steady state has been attained after 460 s. The minimum value of the steady state is equal to 78 °C, while the maximum amounts 80 °C in nominal conditions.

In order to verify the consistency of our model with the experimental studies performed by Pei *et al.*, [11], we have compared the time of reaching set conditions. Figure 12 presents Pei *et al.* experimental results and numerical calculations of the vapour in the turbine's inlet. Figure 13 illustrates Pei *et al.* experimental results and numerical calculations of the R123 refrigerant placed in the condenser's inlet. Experimental studies were conveyed for the rate of heat in the condenser equal to 16 kW [11]. Theoretical model of the ORC cycle has been modified according to the attained results of the experimental studies. The heat load in the model of the condenser has been adjusted to 16 kW level. Figures 11 and 12 prove that parameters in the theoretical model and the experimental studies are similar. The theoretical ORC cycle model reflects the operation of the real working systems and the performed experiment validates this theory.
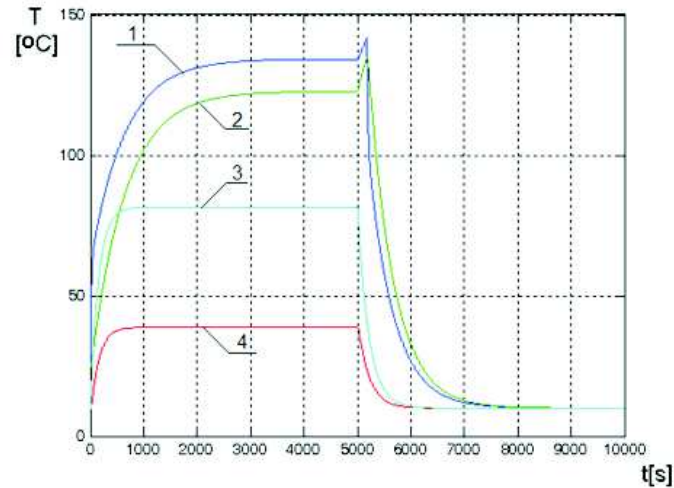
Figure 11. ORC circulation pump failure – temperature calculations (ORC cycle protected): 1 – thermal oil temperature in the evaporator's inlet, 2 – HFE7100 fluid temperature in the evaporator, 3 – HFE7100 fluid temperature in the condenser, 4 – cooling water temperature at the condenser's outlet.
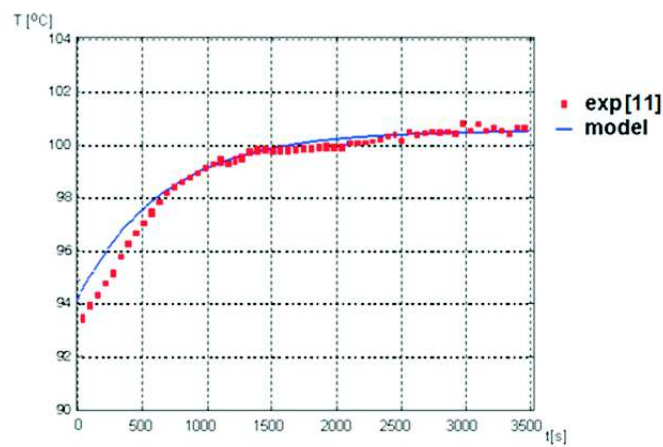

Figure 12. The temperature of refrigerant R123 at the turbine inlet in the theoretical model compared with the temperature value in the experimental one.

4   Summary

The paper presents the issues related to the failure states of the micro-ORC based on the CHP cycle that operates with the condenser evaporator, mi-
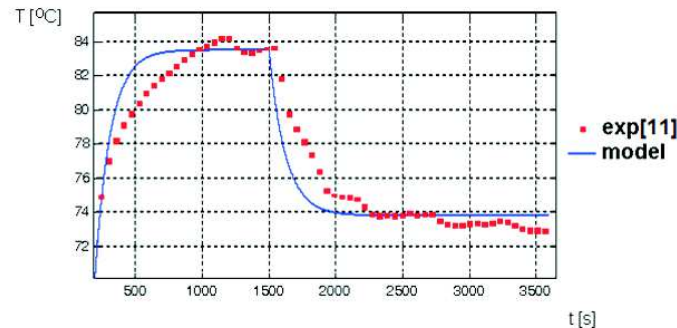
Figure 13. The temperature of the R123 refrigerant in the condenser inlet in the theo-
retical model, compared with the temperature value in the experimental one.

croturbines, pumps and control systems. Failure conditions of the CHP
systems are described by the lumped-parameter models. The proposed
model of the automatically controlled micro-CHP system can predict the
system behaviour in case of any disturbances. It also allows to determine
the inertia of the system in case of failure. The time in which the system
attains the steady state determines the inertia of the system (30 min. to
1 h). The inertia time depends on the mass flow rate (Fig. 10 Exemplary
inertia time). The simulation of failure conditions allowed to define the time
needed for the operating conditions to change into stationary terms. It also
helped to determine the time of the security system response.

Comparing the parameters of our ORC cycle with the parameters ob-
tained in the experimental studies we can conclude that our model illustrates
the operation of the real system. The theoretical model presented above,
faithfully reflects the operation of ORC systems using various working flu-
ids.

References

[1] COLONNA P., PUTTEN H.: *Dynamic modeling of steam power cycles. Part I. Mod-
eling paradigm and validation.* Appl. Therm. Eng. **27**(2007), 467–480.

[2] ORTIZ F.J., GUTIÉRREZ: *Modeling of fire-tube boilers.* Appl. Therm. Eng.
31(2011), 3463–3478.

[3] MATYSKO R.: *The Transient model of ideal refrigeration cycle with control cystem
for heat receiving and intermediary cycle in cooling chamber.* In: HEAT 2011, Proc.

6th Int. Conf. on Transport Phenomena in Multiphase Systems, June 28 – July 2, Ryn 2011.

[4] MIKIELEWICZ J.: *Modelling of thermal-hydraulic processes.* Maszyny Przepływowe, Vol. 17, Ossolineum, Wrocław 1995 (in Polish).

[5] QUOILIN S., AUMANN R., GRILL A., SCHUSTER A., LEMORT V., SPLIETHOFF H.: *Dynamic modeling and optimal control strategy of waste heat recovery.* Appl. Energ. **88**(2011), 2183–2190.

[6] MANENTE G., TOFFOLO A., LAZZARETTO A.,PACI M.: *An organic Rankine cycle off-design model for the search of the optimal control strategy.* Energy **58**(2013), 97–106.

[7] HE Y-L, MEI D-H., TAO W-Q., YANG W-W., LIU H-L.: *Simulation of the parabolic trough solar energy generation system with organic Rankine cycle.* Appl. Energ. **97**(2012), 630–641.

[8] WEI D., LU X., LU Z., GU J.: *Dynamic modeling and simulation of an organic Rankine cycle (ORC) system for waste heat recovery.* Appl. Therm. Eng. **28**(2008), 10, 1216–1224.

[9] ZHANG J.a, ZHANG W., HOU G., FANG F.: *Dynamic modeling and multivariable control of organic Rankine cycles in waste heat utilizing processes.* Comput. Math. Appl. **64**(2012), 5, 908–921.

[10] MATYSKO R., MIKIELEWICZ J.: *Transient model of the combined micro-cogeneration and heat pump cycle.* In: Proc. 1st Int. Cong. on *Thermodynamics*, Poznań 4-7 September, 2011.

[11] PEI G., LI J., LI Y., WANG D., JI J.: *Construction and dynamic test of a small-scale organic Rankine cycle.* Energy **36**(2011), 3215-3223.